Cellular gene delivery via poly(hexamethylene biguanide)/pDNA self-assembled nanoparticles

Alexandru Chivu, PhD[1], Kantaraja Chindera, PhD[2], Graça Mendes[1], Angela An, MD[1], Brian Davidson, MD[1], Liam Good, PhD[2*] and Wenhui Song, PhD[1*]

[1] Centre for Biomaterials in Surgical Reconstruction and Regeneration, Division of Surgery & Interventional Science, University College London, Rowland Hill Street, London NW3 2PF, United Kingdom
[2] Department of Pathology and Population Sciences, Royal Veterinary College, Royal College Street, London NW1 0TU, United Kingdom

*corresponding author: lgood@rvc.ac.uk; w.song@ucl.ac.uk

Abstract

Cellular gene delivery via polycations has wide implications for the potential of gene therapy, but it has remained a challenge due to the plethora of pre- and post-uptake barriers that must be overcome to reach desired efficiency. Herein we report poly(hexamethylene biguanide) (PHMB) as a nano-vector for intracellular delivery of plasmid DNA (pDNA) and oligodeoxynucleotides (ODNs). PHMB and pDNA or ODNs self-assembled into complex nanoparticles at different pH values (7.4 and 12). Their size, charge, cellular uptake, and gene-expression efficiency are assessed and compared to PEI analogues. The systematic results show that the nanoparticles are effective in delivering plasmid DNA and ODNs to model cell lines in culture (HepG2, HEK293T, HeLa), with measurable changes in gene expression levels, comparable to and, in some conditions, even higher than PEI. The well-accepted safety profile of PHMB makes it a valuable candidate for consideration as an effective intracellular DNA vector for further study and potential clinical translation.

Key words: Gene delivery, poly(hexamethylene biguanide) (PHMB), nanoparticles, self-assembly

Introduction

Since the first published use of a cationic polymer for *in vitro* gene delivery[1], there has been a great amount of research focused on developing the strategy as safer substitute for viral vectors[2–5]. Although highly efficient, viruses still generate concern over their potential immunogenicity and they remain very expensive to manufacture. Polycations are the preferred non-viral alternative due to their wide versatility, facile production, low cost, scalability, and low immunogenicity[2,6]. Despite this, toxicity issues remain a problem and their ability to transfect diverse cells with useful efficiencies has not yet reached the same level as that of viral gene delivery, and despite their improved safety profile, this has delayed their translation into clinics.

Nevertheless, since the work of Wu & Wu[1], there has been substantial progress, and other polymers have emerged[7–9], with increased capacity to induce gene expression, such as poly(2-dimethylaminoethyl methacrylate) (PDMAEMA)[10] and poly(N-(2-aminoethylmethacrylamide) (PAEMA)[11]. Polyethyleneimine (PEI) is another example of a cationic polymer, and its continual use and high transfection efficiency in a wide range of model cell lines has made it a benchmark against which new candidates are compared[12,13]. Its use *in vivo* has been limited, but it has become a ubiquitous research tool for *in vitro* transfections and biotechnology applications.

Much of the ongoing research is attempting to identify alternative potential candidates with diverse structures and properties in order to establish a structure-function relationship[14–16], as this appears to correlate with transfection, and may enable the development of cationic polymers with superior transfection rates, comparable to that of viral vectors. Pack *et al.*[17] and Yin *et al.*[2] have reviewed some of the currently accepted functional criteria that an ideal vector must satisfy in order to be considered as a candidate for this application. In brief, the polycation must interact with the nucleic acid, form a stable sub-micron colloidal phase which is efficiently internalised by the target cells, all while protecting the cargo from degrading enzymes. Escaping the endolysosomal compartment via a putative pH-dependent structural change and dissociating upon release into the cytoplasm are widely proposed rate-limiting factors for the success of a vector. However, there is little information on the desirable structural characteristics of a potential carrier, which is why exploring diverse chemical architectures is valuable. So far, the majority of studies have focused on amine-based molecules, containing either primary, secondary, tertiary, quaternary amines, or a mix of these as the charge bearing moieties[2,7–

9,18]. The biguanide functional group has been included in the structure of molecules based on PAMAM dendrimers and they were shown to be effective and safe gene carriers[19], however, to our knowledge, no study up to date has employed it as the single charge bearing moiety.

Herein we report the use of poly(hexamethylene biguanide) (PHMB) as an intracellular vector for plasmid DNA (pDNA) and oligodeoxynucleotides (ODNs). PHMB is an amphiphilic polymer whose repeating unit consists of hydrophobic hexamethylene linked to a hydrophilic biguanide (Figure 1). The biguanide confers the molecule a strongly basic character and is the charge-bearing functional group. PHMB is a well-tolerated and potent antiseptic, preservative, topical disinfectant and active substance in wound dressings[20–23]. Recent work has shown it is capable of self-assembly with nucleic acids[24–26] and small molecules[27] and can deliver them to cells *in vitro*. The present study investigates PHMB's potential as a vector for cellular delivery of DNA, by confirming and quantifying gene expression following delivery of model plasmids. Different self-assembly conditions (pH, PHMB – DNA weight ratios) are also explored in order to optimise these parameters for subsequent use. A comparison of efficiency of DNA uptake and induction of gene expression to the widely used PEI is also provided.

Methods

PHMB hydrochloride (Vantocil™) was obtained from Lonza, and PEI (linear, 25 kDa MW) from Polysciences. Oligodeoxynucleotides (ODNs) and fluorescently labelled ODNs (f-ODNs) were supplied by Eurofins Genomics, with the following sequences: f-ODN 5'-[FITC]-ATCGATGTTTACCTGACCTCATTT-3', ODNs 5'-AACATCATCCCTGCCTCTAC-3'. The plasmid pEGFP-N1 was acquired from NovoPro Labs. Dulbecco's modified eagle medium (DMEM), foetal bovine serum (FBS), penicillin-streptomycin, pCMV-Luciferase plasmid (Cypridina), luciferase assay kit, phosphate buffered saline (PBS), 6X loading dye, deionised water, wheat germ agglutinin Alexa Fluor™ 594 conjugate, trypsin-EDTA, and Prolong™ Diamond Antifade mounting medium were purchased from Life Technologies. Sodium citrate, agarose, heparin, ethidium bromide, 10X TBE buffer, disodium hydrogen phosphate, osmium tetroxide, formaldehyde, Hoechst 33258, sodium azide, and bovine serum albumin (BSA) were purchased from Sigma-Aldrich.

Nanoparticle preparation

The particles were formed via self-assembly, through the electrostatic interaction of two opposite-charge polyelectrolytes in an appropriate pH buffer. For the present work, DNA (pDNA or ODNs) was dissolved in either PBS (pH 7.4) or 25 mM disodium hydrogen phosphate (pH 12), followed by the addition of a solution containing 3 times more polycation (PEI or PHMB) than the amount of DNA present in the initial solution, followed by vigorous mixing. The resulting mix was incubated at room temperature for 15 minutes prior to its use.

Cell culture and maintenance

The cell lines (HepG2, HEK293T, HeLa) were maintained in a humidified atmosphere incubator at 37 °C and 5% CO_2. The culture medium was 1 g/L DMEM supplemented with 10% FBS and 1% penicillin-streptomycin, henceforth referred to as 'complete DMEM'.

Gel permeation chromatography (GPC)

Molecular weight (MW) was measured with an Agilent GPC system equipped with a Sephadex LH-20 column. The column was equilibrated with running buffer (0.1 M citrate pH 4.5 and 0.025% sodium azide). For the measurement, the column was loaded with 200 μL sample, at a concentration of 1 mg/mL in running buffer, and run for 20 minutes at constant flowrate of 5 mL/h at 20 °C. The change in refractive index was monitored with a Wyatt MALS laser light scattering instrument, and the values were used to generate the dn/dc standard curve. The MW was calculated with Astra software.

Gel retardation assay

Plasmid DNA (pEGFP-N1, 200 ng) or ODNs (200 ng) were mixed with the appropriate amounts of PHMB or PEI solutions in PBS, in a final volume of 10 μL. In some cases, heparin was added to DNA solutions, before or after the addition of the polymer. The mixes were incubated at room temperature for 15 minutes, then 2 μL 6X DNA loading dye were added to each. The resulting mixes were loaded onto 1% agarose gel (for pDNA) or 3% agarose gel (for ODNs) containing 0.5 μg/mL ethidium bromide. Electrophoresis was performed for 1 h at 90 V in 0.5X TBE buffer pH 8.3 (45 mM Tris-borate, 1 mM EDTA) using a Bio-Rad Sub-Cell™ electrophoresis apparatus. The gels were imaged with a Syngene G:Box system equipped with a UV transilluminator. The colours were inverted.

ζ potential measurement

Plasmid DNA (pEGFP-N1, 1 µg) or ODNs (1 µg) were added to 1 mL of either pH 7.4 buffer (PBS) or pH 12 buffer (disodium hydrogen phosphate), followed by 3 µg PHMB or PEI. The resulting mix was incubated at room temperature for 15 minutes, then transferred to a folded capillary zeta cell (Malvern). The ζ potential was measured in triplicates using a Malvern Zetasizer Nano ZS90 analyser, averaging 12 runs per measurement.

Dynamic light scattering

Plasmid DNA (pEGFP-N1) or ODNs were mixed with PHMB or PEI in the weight ratio 1:3. The final DNA concentrations were 16 µg/mL, 8 µg/mL, and 4 µg/mL (plasmid), and 3 µg/mL, 1.5 µg/mL (ODNs). The diluent buffers were PBS pH 7.4 (for PEI and PHMB) or 25 mM disodium hydrogen phosphate buffer pH 12 (for PHMB). The mixes were transferred to plastic cuvettes (Sarstedt) and dynamic light scattering (DLS) measurements were performed using a Malvern Nano S90 analyser in 3 cycles of 12 measurements.

Transmission electron microscopy (TEM)

The particles were generated by adding 900 ng PHMB to a solution of 300 ng plasmid DNA (pEGFP-N1) or ODNs in 300 µL buffer at pH 7.4 or pH 12, followed by 15 minutes incubation at room temperature. From this, 20 µL were deposited on the carbon-coated side of a TEM copper grid (Agar Scientific) and the solvent was evaporated at room temperature. The grid was dipped in 1% osmium tetroxide (OsO_4) for 5 seconds and stored in a desiccator until imaging. The TEM equipment was a Jeol 2100 equipped with a 200 keV LaB_6 electron gun.

Assessment of cellular uptake of fluorescently labelled DNA (f-ODNs)

Confocal microscopy: HepG2, HEK293T, and HeLa were seeded in 24-well plates containing 13 mm coverglasses at a density of 2.5×10^4 cells/cm^2 in complete DMEM, and incubated overnight at 37°C and 5% CO_2. The next day, polyplexes were generated by adding 2.4 µg polymer (PHMB or PEI) to 50 µL PBS containing 0.8 µg f-ODNs and incubating at room temperature for 15 minutes. From the resulting mix, 15 µL were then added to corresponding wells containing 1 mL full DMEM and incubated for 24 h. The final polymer concentration per well was 0.7 µg/mL. After the incubation, the cells were fixed with 4% formaldehyde for 20 minutes. The membranes were stained for 20 minutes with 5 µg/mL wheat germ agglutinin Alexa Fluor™ 594 conjugate. The nuclei were stained for 10 minutes with 10

µg/mL Hoechst 33258. The cover glass slips were mounted on rectangular glass slides using ProLong™ Diamond Antifade Mountant and imaged with a Nikon Eclipse Ti confocal microscope.

Flow cytometry: HepG2, HEK293T, and HeLa were seeded in 6-well plates at a density of 2.5×10^4 cells/cm² in complete DMEM and incubated overnight at 37°C and 5% CO_2. The following day, 2.4 µg polymer (PHMB or PEI) were added to 50 µL PBS containing 0.8 µg f-ODNs. The resulting mix was incubated at room temperature for 15 minutes, after which the entire volume was added to corresponding wells containing 2.5 mL complete DMEM. The final polymer concentration per well was 1 µg/mL. The cells were incubated for 24 h at 37°C and 5% CO_2. At the end of the incubation period, the medium was removed, the cells were recovered by trypsinisation (0.25% trypsin-EDTA) and fixed 4% formaldehyde for 20 minutes. Finally, the cells were resuspended in 0.5% BSA in PBS. Flow cytometry was performed using a BD LSR II flow cytometer, and the results were analysed with FlowJo v10 software. The control cell population was gated and the proportion of cells (% total) with higher FITC signal than the control was recorded for each measurement.

Green fluorescent protein expression from pEGFP-N1 after transfection

Polyplexes were generated by mixing 0.8 µg pEGFP-N1 and 2.4 µg polymer (PEI or PHMB) in 50 µL of the corresponding buffer (PBS pH 7.4 or pH 12 buffer) and incubating at room temperature for 15 minutes. Separately, HepG2, HEK293T, and HeLa cells were seeded in 24-well plates at a density of 2.5×10^4 cells/cm² in 1 mL complete DMEM. To these, 15 µL of the corresponding polyplex mixes was added, for a final polymer concentration of 0.7 µg/mL. The cells were incubated for three days at 37°C and 5% CO_2 and visualised with an EVOS FL fluorescence microscope.

Luciferase assay (pCMV-Luciferase transfection)

Polyplexes of pCMV-Luciferase plasmid were generated by mixing 0.4 µg plasmid with 1.2 µg PEI or PHMB in 100 µL of the corresponding buffer (PBS pH 7.4 for PEI and pH 12 buffer for PHMB) and incubating at room temperature for 15 minutes. Separately, HepG2, HEK293T, and HeLa were seeded in 96-well plates at a density of 5×10^4 cells/cm² in 250 µL complete DMEM (n=4 per condition). To each well, 10 µL of the corresponding polyplex mix were added, for a final polymer concentration of 1 µg/mL. The cells were incubated for three days at 37°C and 5% CO_2. At the end of the incubation period, the amount of secreted luciferase was quantified using a luciferase assay kit as per the

manufacturer's instructions. The luminescence was measured with a Tecan Infinite M200 Pro plate reader in black flat-bottom 96-well plates. The assay was repeated 3 times.

Measurement of cellular viability (PrestoBlue™ assay)

HepG2, HEK293T, and HeLa were seeded in 48-well plates at a density of 2.0×10^4 cells/cm^2 in complete DMEM. An equal volume of complete DMEM containing 2X polymer concentration (PEI or PHMB) was added to each corresponding well (n=6 per concentration). The final polymer concentration range was 0.25 – 5 µg/mL. The reagent manufacturer's instructions were followed. The fluorescence of the wells was measured (excitation 530 nm, emission 620 nm) using a Fluoroskan Ascent FL plate reader. After subtracting the blank (10% PrestoBlue reagent in complete DMEM), the cell viability was calculated as a percentage relative to the control samples (cells grown in complete DMEM).

Statistical analysis

GraphPad Prism software v7 was used to perform statistical analyses. Data was presented as mean ±standard deviation. P values were generated by either t-tests or one-way ANOVA, and considered significant when $p < 0.05$.

Results

Gel permeation chromatography

The average molecular weight of the commercial PHMB samples used in this study was determined to be 3300 Da, with a polydispersity index of 1.9 (Figure S1, Table S1 in Supplementary Information).

Gel retardation assay

PHMB, like PEI, interacts with both pDNA and ODNs in a ratio-dependent manner, as evidenced by the fading out of the DNA bands in Figure 2 (A, B), as the ratio of polymer to DNA is increased. The negative charge of pDNA is neutralised at polymer to DNA ratios above 3 (weight/weight), and in the case of PHMB, this happens whether the interaction occurred at pH 7.4 or 12 (Figure 2 B). A similar behaviour is observed for ODNs interacting with PHMB whereby ratios higher than 3 are enough to neutralise at either pH 7.4 or pH 12. This was not the case for PEI, for which ODNs were not fully neutralised for any of the tested polymer:DNA weight ratios (1-6, Figure 2A).

In the heparin-exclusion assays shown in figure 2 (C-E), heparin replaces both pDNA and ODNs in the PHMB polyplexes whether these were assembled at pH 7.4 or 12 (only 7.4 was tested for ODNs). This was indicated by the increase in the intensity of DNA bands as the amount of heparin relative to DNA increases. It was observed that this exclusion behaviour of heparin occurred whether heparin was present before or after the PHMB-DNA polyplex formation, although slightly more pronounced in the former case (intensity of DNA bands). Heparin did not trigger the release of pDNA from PEI polyplexes for the ratios tested here (Figure 2F).

ζ potential

The results for the ζ potential measurements are summarised in Table 1. All values for DNA polyplexes with PHMB were positive at both pH 7.4 and pH 12, although the magnitude was lower for the particles formed at pH 12. Similarly, the polyplexes of DNA with PEI were also of positive magnitude at pH 7.4. Measurements of PEI polyplexes at pH 12 were not performed.

Dynamic light scattering

DLS measurements showed that for constant concentrations of PHMB and DNA, the polyplexes self-assembled at pH 12 had a smaller hydrodynamic diameter than those formed at pH 7.4 (Table 2 and Figure S2 A-B SI). Also, for constant pH and PHMB:DNA ratio, the lower concentrations used in this study generated smaller particles than the higher concentrations. This was the case for both pDNA (Figure S2 A, C SI) and ODNs (Figure S2 B, D SI). Similar behaviour was observed for PEI, albeit measurements for it were only performed at pH 7.4 (Figure S2 C-D SI). At pH 7.4 the plasmid polyplexes with PHMB (Figure S2 A SI) were larger than those for PEI (Figure S2 C), whereas the ODN polyplexes for the two polymers were of similar size (Figure S2 B, D SI). It is of note that the plasmid polyplexes with PHMB at pH 12 were slightly smaller than the PEI particles at pH 7.4 in the concentration of 16 µg/mL, but larger than those in the concentration of 8 and 4 µg/mL, whereas the ODN polyplexes at pH 12 were smaller than those for PEI at pH 7.4 (Table 2). The particles were monodispersed and their corresponding hydrodynamic diameters and PDI values are shown in Table 2.

Transmission electron microscopy

8

TEM imaging revealed the formation of submicron particles with round morphology (Figure 3). The particle diameter was larger for the polyplexes of the higher molecular weight DNA (plasmid) relative to the ones of the lower MW ODNs. It was also apparent that the particles formed at pH 12 were smaller than those assembled at pH 7.4.

Cellular uptake of f-ODNs

Polyplexes of f-ODNs with PHMB showed positive cellular uptake after 24 hours, with punctiform cytoplasmic distribution of the fluorescence signal in the three cell lines tested (Figure 4 A). The green fluorescence signal was also localised in the nuclear space (less intense for HeLa than for the other two cell lines), suggesting release of the particles from the encapsulating uptake vesicles. In contrast to PHMB, the PEI polyplexes showed no obvious uptake of the f-ODNs under the same conditions tested. This qualitative observation was confirmed quantitatively by flow cytometry analysis (Figure 4 B), where f-ODNs polyplexes with PHMB were shown to be up taken to greater extent by all three cell lines after 24 hours, judging by the intensity and proportion of fluorescent cells, when compared to those with PEI. This was the case whether the polyplex self-assembly occurred at pH 7.4 or 12. The PHMB particles generated at pH 7.4 produced higher proportion of fluorescent cells (77.4 ±7.6% HepG2, 81 ±10.2% HEK293T , 65.5 ±15.3% HeLa) than those at pH 12 (36.7 ±5.9% HepG2, 32.4±9.1% HEK293T, 29.3 ±17.2% HeLa), and both significantly higher than PEI at pH 7.4 (7.6 ±1.3% HepG2, 10.2 ±3.2% HEK293T, 4.1 ±2.3% HeLa).

Green fluorescent protein expression

PHMB, like PEI, delivered pEGFP-N1 plasmid to HEK293T and HeLa and elicited expression of green fluorescent protein (GFP), as evidenced by the green signal in Figure 5 A. This only occurred when the PHMB polyplexes self-assembled at pH 12, but not at pH 7.4. There was no detectable GFP expression for HepG2 for either of the two delivery vectors used here.

Luciferase assay

The complex of PHMB with the plasmid pCMV-Luc assembled at pH 12 showed a higher level of luciferase expression than the PEI analogue assembled at pH 7.4 in both HEK293T and HeLa cell lines (Figure 5 B). The mean luminescence signal produced by luciferase expression also appeared higher in HepG2, but the difference was not significant.

Cellular viability

Both PEI and PHMB exhibited similar dose-dependent decrease trends in cellular viability for HEK293T and HeLa cells, as measured via PrestoBlue™ assay (Figure 6), in the range of concentrations tested here (0.25 – 5 µg/mL). The trend was different for HepG2, for which only PHMB produced a statistically significant decrease in viability above 1.5 µg/mL.

Discussion

The average molecular weight of the PHMB sample used in this study was 3300 Da, which is consistent with reported literature molecular weights for commercial PHMB between 2400 Da and 4200 Da, suggesting an average theoretical degree of polymerisation n = 12. However, de Paula and co-workers[28] argue that the contribution of end groups cannot be neglected given the relatively low molecular weight of the polymer. Therefore, they concluded an average n = 6.5 is more plausible, which is in the appropriate range for DNA condensation[29]. The molecular weight distribution is governed by an equilibrium between the rate of polymer chain extension and the thermal breaking of the biguanide group due to the high temperatures employed during the polycondensation reaction for its large-scale production[30,31]. The breaking occurs randomly in the chain, generating the large polydispersity index of 1.9 in the case of the present sample. The relatively high PDI for PHMB was not detrimental for its function in the present study, nor others it is currently employed in. Should a monodisperse distribution of molecular weights ever be required for future applications, a new controlled polymerisation method would have to be developed. For instance, the high activation energies of the nitrile groups could be overcome by increasing their polarity with the use of Lewis acids and thus their propensity for amine nucleophilic attack, allowing for polycondensation in more mild temperature conditions and prevent thermal chain breaking.

Under aqueous, physiological conditions, biguanides in their iminic form (Figure 7 A-a, erroneously represented in the literature as the aminic form in Figure 7 A-b) participate in acid-base proton exchange[32], resulting in the mesomeric form (Figure 7 A-c). This species is stabilised by six resonance contributors (Figure 7 A-d), leading to the positive charge being delocalised over the entire chemical group, accounting for its high proton affinity[33] and strong basic character[34] ($pK_a \approx 12$). This strong basic character renders PHMB fully protonated at physiological pH, allowing it to interact electrostatically with the negatively charged backbone of nucleic acids. It also implies that the positive

charge is maintained on the chain backbone across a wide range of pH values, up to and including pH 12, where only approximately 50% of the biguanides are protonated (Henderson-Hasselbalch relationship)[35]. PHMB, like PEI, interacts with DNA in a ratio-dependent manner, neutralising charge through random interactions between the charged sites of the two polyelectrolytes. This occurs for weight ratios above 3, as evidenced by the electrophoretic mobility shift assay in figure 2 A-B. Given the large molecular weight difference between the two chemical species (plasmid MW ≈ 2925 kDa, PHMB MW ≈ 3.3 kDa), multiple PHMB molecules are required for complete neutralisation of each plasmid. It has been proposed[36] that this occurs via the formation of inter- and intramolecular PHMB bridges between DNA molecules, ultimately resulting in condensation of the DNA/PHMB complex (polyplex) and formation of a particle suspension. The relative proportion of the two polyelectrolytes influences the ratio of the two types of possible bridges, and ultimately size of the suspended particles. This is exemplified in figure 7 B.

A high ratio ensures not only neutralisation of the DNA, but also provides sufficient excess charge to generate positively charged particles, which have been associated with good cellular uptake[37]. All particles produced in this study via self-assembly of PHMB with DNA in a weight ratio 3:1 showed positive ζ potentials (Table 1) with a higher magnitude at pH 7.4 than at pH 12 due to a higher proportion of positively charged biguanide sites at the lower pH. The measurement for PEI was only performed at pH 7.4 due to PEI's low pK_a value implying lack of positive charge at pH values approaching 12[38]. The pH 12 PHMB particles could possess lower long-term stability and a higher potential for aggregation than the pH 7.4 ones[39,40], but in this study, they were used immediately following their self-assembly. A high enough ratio of polycation to fully neutralise, condense and tightly pack the DNA is also favourable because it minimises the access to the DNA of potential nucleases present in the biological environment, thus preventing its enzymatic degradation. In the case of PHMB, it is presumed that the hexamethylene groups also interact with the nitrogenous bases of DNA via hydrophobic interactions[41,42], further increasing the binding strength between the two polyelectrolytes, and the compactness of the polyplex.

The tendency of the particle size to decrease with the increase in pH during self-assembly, as per the DLS measurements (Table 2, Figure S2 SI), is due to the reduction in the degree of protonation of PHMB, and thus in the potential number of positively charged sites available for bridging between DNA molecules. Lower concentrations also generate smaller particles because of the lowered chance of

PHMB chains encountering multiple DNA molecules during the polyelectrolytes neutralisation, thus favouring inter- to intramolecular bridging of DNA by PHMB.

The polyplex formation of DNA and PHMB was further confirmed by transmission electron microscopy (Figure 3). The relative dispersity of sizes likely arises due to the heterogeneity in molecular weights of the PHMB chains, producing different degrees of bridging of DNA. However, the different sized particles remain submicron, with potential for cellular internalisation. Whereas it has been reported[43,44] that non-phagocytic cells preferentially uptake small particles ranging between 20 - 50 nm, there is also evidence of uptake of particles up to 1 μm[45,46]. The cut-off particle size for efficient cellular internalisation is heterogeneous and dependent on the type of cell and physicochemical characteristics of the colloid and the biological environment[47]. Both PEI and PHMB polyplexes assembled at pH 7.4 exhibit ζ potentials favourable for stability and cellular uptake. Their sizes vary with concentration, pH, and DNA MW, but these can be optimised to produce hydrodynamic diameters within literature-reported values for positive cellular internalisation, such as the ones exhibited by the lowest DNA concentrations in Table 2.

We have shown positive intracellular uptake of f-ODNs via PHMB after 24 hours incubation (Figure 4 A) in HepG2, HeLa, and HEK293T. Alongside the punctate cytoplasmic distribution of the green fluorescence signal, which is likely due to DNA internalised in endosomal vesicles, there is also some indication of uniform diffuse fluorescence. This could suggest not only endosomal release of the polyplexes, but also their dissociation and DNA release in the cytoplasmic and nuclear space. The mechanism for the transport of the DNA in the nucleus is not yet clear, but it is possible that the breaking down of the nuclear membrane during mitosis could allow for free diffusion and accumulation of f-ODNs[48,49]. The dissociation of the DNA from the polyplex in the cytoplasm could occur because of competition of negatively charged cytoplasmic molecules for the positively charged sites of PHMB, as suggested by the heparin-exclusion assay whereby negatively charged heparin promoted the release of DNA from the complex (Figure 2 C-D). The low molecular weight of PHMB could play a role in this rapid dissociation given that the disassembly of polyplexes formed by the higher molecular weight PEI was not triggered by the same amounts of heparin (Figure 2 F).

In contrast to PHMB, the PEI group showed no obvious uptake of f-ODNs under the same conditions tested (Figure 4 A), despite its well-known capacity to act as a DNA vector[13]. This qualitative

observation was confirmed quantitatively by flow cytometry (Figure 4 B-C), where f-ODNs were shown to be uptaken to greater extent by all three cell lines after 24 hours incubation when bound by PHMB, compared to PEI. This was the case whether the PHMB and f-ODNs self-assembly occurred at pH 7.4 or pH 12. The PHMB polyplexes generated at pH 7.4 produced higher uptake of the f-ODNs than those at pH 12, due to the higher relative density of positive charge on PHMB at the lower pH, allowing for binding of more f-ODNs. The incomplete neutralisation of ODNs by PEI (Figure 2A) at ratios sufficiently high to otherwise neutralise plasmid DNA (Figure 2B) could also account for this discrepancy.

Although uptake of ODNs by PHMB was confirmed by confocal microscopy and flow cytometry following self-assembly at pH 7.4, transfection of pEGFP-N1 plasmid at this pH produced no noticeable expression of GFP (Figure 5 A). However, transfection of pEGFP-N1 via PHMB at pH 12 generated a GFP signal comparable to that by PEI at pH 7.4 (Figure 5 A). The difference in particle size at the two different pH levels (Figure 3 A) could account for a variation in uptake and subsequent gene expression for the PHMB-plasmid polyplexes. Uptake of plasmid at pH 7.4 has not yet been confirmed, and this remains to be ascertained via confocal microscopy studies of fluorescently labelled plasmid DNA. Alternatively, a potentially lower degree of interaction between the two polyelectrolytes (PHMB, plasmid DNA) at pH 12 relative to pH 7.4, due to a decrease in positive charge density on PHMB with increase in pH [35,50], could generate looser, less compact particles, for which intracellular dissociation and DNA release might be more likely. This might explain the difference in gene expression between particles self-assembled at the two pH levels. However, under the experimental conditions tested here, no difference in behaviour was observed in the heparin exclusion assays between PHMB polyplexes produced at either pH 7.4 or pH 12 (Figure 2 D, E), so the cause ultimately remains unclear. Lack of detectable GFP expression was evident for HepG2, but its difficulty in being transfected is well-known [51].

The expression of luciferase following transfection of pCMV-Luc plasmid was quantitatively higher when using PHMB (pH 12) as vector than when using PEI (pH 7.4), in both HeLa and HEK293T (Figure 5 B). The mean luminescence signal produced by luciferase expression also appeared higher in HepG2, but the difference was not significant. The transfection success of PHMB in the present work suggests that the endosomal pH-buffering capacity of the carrier is not a requirement for positive transfection, although the efficiency of PEI has been attributed to its ability to resist endosome acidification. PHMB is a strong base for which the pK_a is much larger than the endosomal pH, so it is unable to prevent its

acidification and trigger osmotic lysis, as proposed by Behr and colleagues in the 'proton sponge' hypothesis[52], and which has served as an important criterion for the design of new potential carriers. Moreover, Funhoff and colleagues[53] noted low transfection potential for carriers possessing endosomal-buffering capacities, which further emphasises our proposition.

Even though they pose fewer risks than viral carriers, a major limitation of polycations is also their cytotoxicity[54], as measured *in vitro* by a decrease in cellular viability (Figure 6). This occurs due to their electrostatic interaction with the cellular membrane and initiation of membrane damage and increased permeability[55]. The extent of this damage is dependent on the molecular weight and charge density of the polycation, but also on the polymer concentration and the cell type. The dose-dependent cytotoxic behaviour of PEI is already well-established[56] and was anticipated. Also, given that the antibacterial effect of PHMB is partly based on its ability to interact with negatively charged lipid bilayers[57,58], a negative effect at high concentrations is to be expected. The *in vitro* cell toxicity can often be misleading and not representative of the *in vivo* behaviour, given that PHMB has a long history of safe use in the clinics[22]. Dosage can be optimised for both polymers to reduce negative effects, and this was considered and adjusted when comparing them in the current work, such that there be no decrease in cell viability during any assay.

We show that the widely used antiseptic polymer PHMB can bind DNA in a wide range of pH conditions, and form condensed submicron particles that can be up taken by HepG2, HEK293T and HeLa cells lines *in vitro,* in serum-rich environments. Gene expression from transfected plasmids was observed in all three cell lines following plasmid delivery by PHMB, for which the transfection efficiency was dependent on the self-assembly pH. Gene expression was observed only in the polyplex groups assembled at pH 12, and not pH 7.4, perhaps due to formation of less compact particles more prone to intracellular dissociation. Under these conditions, PHMB induced similar (in HepG2) or even higher (in HEK293T and HeLa) levels of luciferase expression than the widely used PEI. The present results would suggest that the potential for endosomal pH-buffering of the DNA carrier, as suggested by the 'proton sponge hypothesis' would not be a suitable singular criterion for the exclusion of new potential candidate vectors for gene delivery, as we offer a counterexample for this model. As PHMB was able to also promote the intracellular uptake of low molecular weight DNA, we anticipate positive results in its use for siRNA delivery, as demonstrated by Tirella and colleagues[59]. We therefore propose PHMB,

a polycation with a long history of safe clinical use, as a viable candidate for gene delivery, with relevance for study for potential future clinical translation.

Conflict of interest: Liam Good and Kantaraja Chindera are coinventors on a patent describing gene delivery via polymeric biguanides (US20140242097A1).

References

[1]   G.Y. Wu, C.H. Wu, Receptor-mediated in vitro gene transformation by a soluble DNA carrier system., J. Biol. Chem. 262 (1987) 4429–32. http://www.ncbi.nlm.nih.gov/pubmed/3558345 (accessed April 15, 2019).

[2]   H. Yin, R.L. Kanasty, A.A. Eltoukhy, A.J. Vegas, J.R. Dorkin, D.G. Anderson, Non-viral vectors for gene-based therapy, Nat. Rev. Genet. 15 (2014) 541–555. https://doi.org/10.1038/nrg3763.

[3]   C.L. Hardee, L.M. Arévalo-Soliz, B.D. Hornstein, L. Zechiedrich, Advances in Non-Viral DNA Vectors for Gene Therapy., Genes (Basel). 8 (2017). https://doi.org/10.3390/genes8020065.

[4]   Y. Cheng, R.C. Yumul, S.H. Pun, Virus-Inspired Polymer for Efficient In Vitro and In Vivo Gene Delivery, Angew. Chemie Int. Ed. 55 (2016) 12013–12017. https://doi.org/10.1002/anie.201605958.

[5]   M. Ramamoorth, A. Narvekar, Non viral vectors in gene therapy- an overview., J. Clin. Diagn. Res. 9 (2015) GE01-6. https://doi.org/10.7860/JCDR/2015/10443.5394.

[6]   L. Li, Y. Wei, C. Gong, Polymeric Nanocarriers for Non-Viral Gene Delivery, J. Biomed. Nanotechnol. 11 (2015) 739–770. https://doi.org/10.1166/jbn.2015.2069.

[7]   Y. Xiang, N.N.L. Oo, J.P. Lee, Z. Li, X.J. Loh, Recent development of synthetic nonviral systems for sustained gene delivery, Drug Discov. Today. 22 (2017) 1318–1335. https://doi.org/10.1016/J.DRUDIS.2017.04.001.

[8]   M.A. Mintzer, E.E. Simanek, Nonviral Vectors for Gene Delivery, Chem. Rev. 109 (2009) 259–302. https://doi.org/10.1021/cr800409e.

[9]   S.K. Samal, M. Dash, S. Van Vlierberghe, D.L. Kaplan, E. Chiellini, C. van Blitterswijk, L. Moroni, P. Dubruel, Cationic polymers and their therapeutic potential, Chem. Soc. Rev. 41 (2012) 7147. https://doi.org/10.1039/c2cs35094g.

[10]   S. Agarwal, Y. Zhang, S. Maji, A. Greiner, PDMAEMA based gene delivery materials, Mater. Today. 15 (2012) 388–393. https://doi.org/10.1016/S1369-7021(12)70165-7.

[11]   Y. Wu, M. Wang, D. Sprouse, A.E. Smith, T.M. Reineke, Glucose-Containing Diblock Polycations Exhibit Molecular Weight, Charge, and Cell-Type Dependence for pDNA Delivery, Biomacromolecules. 15 (2014) 1716–1726. https://doi.org/10.1021/bm5001229.

[12]   X. Wang, D. Niu, C. Hu, P. Li, Polyethyleneimine-Based Nanocarriers for Gene Delivery, (n.d.). https://www.ingentaconnect.com/content/ben/cpd/2015/00000021/00000042/art00009 (accessed May 11, 2019).

[13]   A.P. Pandey, K.K. Sawant, Polyethylenimine: A versatile, multifunctional non-viral vector for nucleic acid delivery, Mater. Sci. Eng. C. 68 (2016) 904–918. https://doi.org/10.1016/J.MSEC.2016.07.066.

[14]   M.E. Hwang, D.W. Pack, Elucidating Structure-Function Relationship of Primary Amines in

Cationic Polymer Gene Delivery Vehicles, Mol. Ther. 17 (2009) S337.

https://doi.org/10.1016/S1525-0016(16)39241-3.

[15]   D.J. Chen, B.S. Majors, A. Zelikin, D. Putnam, Structure–function relationships of gene

delivery vectors in a limited polycation library, J. Control. Release. 103 (2005) 273–283.

https://doi.org/10.1016/J.JCONREL.2004.11.028.

[16]   H. Xing, M. Lu, T. Yang, H. Liu, Y. Sun, X. Zhao, H. Xu, L. Yang, P. Ding, Structure-function

relationships of nonviral gene vectors: Lessons from antimicrobial polymers, Acta Biomater. 86

(2019) 15–40. https://doi.org/10.1016/J.ACTBIO.2018.12.041.

[17]   D.W. Pack, A.S. Hoffman, S. Pun, P.S. Stayton, Design and development of polymers for gene

delivery, Nat. Rev. Drug Discov. 4 (2005) 581–593. https://doi.org/10.1038/nrd1775.

[18]   E. Keles, Y. Song, D. Du, W.-J. Dong, Y. Lin, Recent progress in nanomaterials for gene

delivery applications, Biomater. Sci. 4 (2016) 1291–1309.

https://doi.org/10.1039/C6BM00441E.

[19]   H. Xing, L. Cheng, M. Lu, H. Liu, L. Lang, T. Yang, X. Zhao, H. Xu, L. Yang, P. Ding, A

biodegradable poly (amido amine) based on the antimicrobial polymer polyhexamethylene

biguanide for efficient and safe gene delivery, Colloids Surfaces B Biointerfaces. 182 (2019)

110355.

[20]   C. Martín-Trapero, M. Martín-Torrijos, L. Fernández-Conde, M. Torrijos-Torrijos, E. Manzano-

Martín, J.L. Pacheco-del Cerro, L.I. Díez-Valladares, Surgical site infections. Effectiveness of

polyhexamethylene biguanide wound dressings., Enferm. Clin. 23 (2013) 56–61.

https://doi.org/10.1016/j.enfcli.2013.01.005.

[21]   J.C. Dumville, T.A. Gray, C.J. Walter, C.A. Sharp, T. Page, R. Macefield, N. Blencowe, T.K.

Milne, B.C. Reeves, J. Blazeby, Dressings for the prevention of surgical site infection,

Cochrane Database Syst. Rev. (2016). https://doi.org/10.1002/14651858.CD003091.pub4.

[22]   S. Gilliver, PHMB: a well-tolerated antiseptic with no reported toxic effects, J. Wound Care.

(2009).

[23]   A. Worsley, K. Vassileva, J. Tsui, W. Song, L. Good, A. Worsley, K. Vassileva, J. Tsui, W.

Song, L. Good, Polyhexamethylene Biguanide: Polyurethane Blend Nanofibrous Membranes for Wound Infection Control, Polymers (Basel). 11 (2019) 915. https://doi.org/10.3390/polym11050915.

[24]   K. Chindera, M. Mahato, A. Kumar Sharma, H. Horsley, K. Kloc-Muniak, N.F. Kamaruzzaman, S. Kumar, A. McFarlane, J. Stach, T. Bentin, L. Good, The antimicrobial polymer PHMB enters cells and selectively condenses bacterial chromosomes, Sci. Rep. 6 (2016) 23121. https://doi.org/10.1038/srep23121.

[25]   R. Firdessa, L. Good, M.C. Amstalden, K. Chindera, N.F. Kamaruzzaman, M. Schultheis, B. Röger, N. Hecht, T.A. Oelschlaeger, L. Meinel, T. Lühmann, H. Moll, Pathogen- and Host-Directed Antileishmanial Effects Mediated by Polyhexanide (PHMB), PLoS Negl. Trop. Dis. 9 (2015) e0004041. https://doi.org/10.1371/journal.pntd.0004041.

[26]   L. Good, K. Chindera, V. Gburcik, Methods for promoting entry of an agent into a cell, US Patent 10238683 B2, 2019.

[27]   N. Kamaruzzaman, M. Pina, A. Chivu, L. Good, N.F. Kamaruzzaman, M.D.F. Pina, A. Chivu, L. Good, Polyhexamethylene Biguanide and Nadifloxacin Self-Assembled Nanoparticles: Antimicrobial Effects against Intracellular Methicillin-Resistant Staphylococcus aureus, Polymers (Basel). 10 (2018) 521. https://doi.org/10.3390/polym10050521.

[28]   G.F. De Paula, G.I. Netto, L.H.C. Mattoso, G.F. De Paula, G.I. Netto, L.H.C. Mattoso, Physical and Chemical Characterization of Poly(hexamethylene biguanide) Hydrochloride, Polymers (Basel). 3 (2011) 928–941. https://doi.org/10.3390/polym3020928.

[29]   I. Koltover, K. Wagner, C.R. Safinya, DNA condensation in two dimensions, Proc. Natl. Acad. Sci. U. S. A. 97 (2000) 14046. https://doi.org/10.1073/PNAS.97.26.14046.

[30]   G.C. East, J.E. McIntyre, J. Shao, Polybiguanides: synthesis and characterization of polybiguanides containing hexamethylene groups, Polymer (Guildf). 38 (1997) 3973–3984. https://doi.org/10.1016/S0032-3861(96)00969-X.

[31]   F. Rose, G. Swain, US Patent No. 2,643,232 - Polymeric Diguanides, 1953.

[32]   * Prasad V. Bharatam, and Dhilon S. Patel, P. Iqbal, Pharmacophoric Features of Biguanide

Derivatives: An Electronic and Structural Analysis, (2005). https://doi.org/10.1021/JM050602Z.

[33] Z.B. Maksić, B. Kovačević, Absolute Proton Affinity of Some Polyguanides, (2000). https://doi.org/10.1021/JO991592A.

[34] F. Kurzer, E.D. Pitchfork, The chemistry of biguanides, in: Biguanides, Springer-Verlag, Berlin/Heidelberg, 1968: pp. 375–472. https://doi.org/10.1007/BFb0050853.

[35] A.G. Hills, pH and the Henderson-Hasselbalch equation, Am. J. Med. 55 (1973) 131–133.

[36] M.J. Allen, A.P. Morby, G.F. White, Cooperativity in the binding of the cationic biocide polyhexamethylene biguanide to nucleic acids, Biochem. Biophys. Res. Commun. 318 (2004) 397–404. https://doi.org/10.1016/J.BBRC.2004.04.043.

[37] C. Foged, B. Brodin, S. Frokjaer, A. Sundblad, Particle size and surface charge affect particle uptake by human dendritic cells in an in vitro model, Int. J. Pharm. 298 (2005) 315–322. https://doi.org/10.1016/J.IJPHARM.2005.03.035.

[38] X. Zhang, D. Taylor, R. Thomas, J. Penfold, I. Tucker, Modifying the adsorption properties of anionic surfactants onto hydrophilic silica using the pH dependence of the polyelectrolytes PEI, ethoxylated PEI, and polyamines, Langmuir. 27 (2011) 3569–3577.

[39] V. Gallardo, M.E. Morales, M.A. Ruiz, A. V Delgado, An experimental investigation of the stability of ethylcellulose latex: Correlation between zeta potential and sedimentation, Eur. J. Pharm. Sci. 26 (2005) 170–175. https://doi.org/https://doi.org/10.1016/j.ejps.2005.05.008.

[40] I. Ostolska, M. Wiśniewska, Application of the zeta potential measurements to explanation of colloidal Cr 2 O 3 stability mechanism in the presence of the ionic polyamino acids, Colloid Polym. Sci. 292 (2014) 2453–2464.

[41] I.S. Kikuchi, A.M. Carmona-Ribeiro, Interactions between DNA and Synthetic Cationic Liposomes, J. Phys. Chem. B. 104 (2000) 2829–2835. https://doi.org/10.1021/jp9935891.

[42] D. Matulis, I. Rouzina, V.A. Bloomfield, Thermodynamics of Cationic Lipid Binding to DNA and DNA Condensation: Roles of Electrostatics and Hydrophobicity, J. Am. Chem. Soc. 124 (2002) 7331–7342. https://doi.org/10.1021/ja0124055.

[43] W. Jiang, B.Y.S. Kim, J.T. Rutka, W.C.W. Chan, Nanoparticle-mediated cellular response is

size-dependent, Nat. Nanotechnol. 3 (2008) 145–150. https://doi.org/10.1038/nnano.2008.30.

[44] B.D. Chithrani, A.A. Ghazani, W.C.W. Chan, Determining the Size and Shape Dependence of Gold Nanoparticle Uptake into Mammalian Cells, (2006). https://doi.org/10.1021/NL052396O.

[45] A. Musyanovych, J. Dausend, M. Dass, P. Walther, V. Mailänder, K. Landfester, Criteria impacting the cellular uptake of nanoparticles: A study emphasizing polymer type and surfactant effects, Acta Biomater. 7 (2011) 4160–4168. https://doi.org/10.1016/J.ACTBIO.2011.07.033.

[46] W. Zauner, N.A. Farrow, A.M.. Haines, In vitro uptake of polystyrene microspheres: effect of particle size, cell line and cell density, J. Control. Release. 71 (2001) 39–51. https://doi.org/10.1016/S0168-3659(00)00358-8.

[47] S. Zhang, H. Gao, G. Bao, Physical Principles of Nanoparticle Cellular Endocytosis, ACS Nano. 9 (2015) 8655–8671. https://doi.org/10.1021/acsnano.5b03184.

[48] J. Suh, D. Wirtz, J. Hanes, Efficient active transport of gene nanocarriers to the cell nucleus, Proc. Natl. Acad. Sci. 100 (2003) 3878–3882. https://doi.org/10.1073/PNAS.0636277100.

[49] E.A. Nigg, N. Somia, Nucleocytoplasmic transport: signals, mechanisms and regulation, Nature. 386 (1997) 779–787. https://doi.org/10.1038/386779a0.

[50] Y. Shin, J.E. Roberts, M.M. Santore, The relationship between polymer/substrate charge density and charge overcompensation by adsorbed polyelectrolyte layers, J. Colloid Interface Sci. 247 (2002) 220–230.

[51] M. Cemazar, I. Hreljac, G. Sersa, M. Filipic, Construction of EGFP Expressing HepG2 Cell Line Using Electroporation, in: World Congr. Med. Phys. Biomed. Eng. Sept. 7-12, 2009, Munich, Ger., 2009: pp. 128–131.

[52] J.-P. Behr, The Proton Sponge: a Trick to Enter Cells the Viruses Did Not Exploit, Chim. Int. J. Chem. 51 (1997) 34–36. https://www.ingentaconnect.com/content/scs/chimia/1997/00000051/F0020001/art00026 (accessed May 31, 2019).

[53] A.M. Funhoff, C.F. van Nostrum, G.A. Koning, N.M.E. Schuurmans-Nieuwenbroek, D.J.A.

Crommelin, W.E. Hennink, Endosomal escape of polymeric gene delivery complexes is not always enhanced by polymers buffering at low pH, Biomacromolecules. 5 (2004) 32–9. https://doi.org/10.1021/bm034041+.

[54] B.D. Monnery, M. Wright, R. Cavill, R. Hoogenboom, S. Shaunak, J.H.G. Steinke, M. Thanou, Cytotoxicity of polycations: Relationship of molecular weight and the hydrolytic theory of the mechanism of toxicity, Int. J. Pharm. 521 (2017) 249–258. https://doi.org/10.1016/J.IJPHARM.2017.02.048.

[55] S. Hong, P.R. Leroueil, E.K. Janus, J.L. Peters, M.-M. Kober, M.T. Islam, B.G. Orr, J.R. Baker, M.M. Banaszak Holl, Interaction of Polycationic Polymers with Supported Lipid Bilayers and Cells: Nanoscale Hole Formation and Enhanced Membrane Permeability, Bioconjug. Chem. 17 (2006) 728–734. https://doi.org/10.1021/bc060077y.

[56] V. Kafil, Y. Omidi, Cytotoxic impacts of linear and branched polyethylenimine nanostructures in a431 cells., Bioimpacts. 1 (2011) 23–30. https://doi.org/10.5681/bi.2011.004.

[57] T. Ikeda, A. Ledwith, C.H. Bamford, R.A. Hann, Interaction of a polymeric biguanide biocide with phospholipid membranes, Biochim. Biophys. Acta - Biomembr. 769 (1984) 57–66. https://doi.org/10.1016/0005-2736(84)90009-9.

[58] P. Broxton, P.M. Woodcock, F. Heatley, P. Gilbert, Interaction of some polyhexamethylene biguanides and membrane phospholipids in *Escherichia coli*, J. Appl. Bacteriol. 57 (1984) 115–124. https://doi.org/10.1111/j.1365-2672.1984.tb02363.x.

[59] A. Tirella, K. Kloc-Muniak, L. Good, J. Ridden, M. Ashford, S. Puri, N. Tirelli, CD44 targeted delivery of siRNA by using HA-decorated nanotechnologies for KRAS silencing in cancer treatment, Int. J. Pharm. 561 (2019) 114–123. https://doi.org/10.1016/j.ijpharm.2019.02.032.
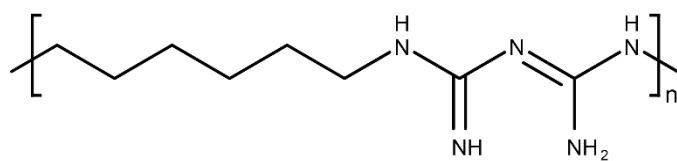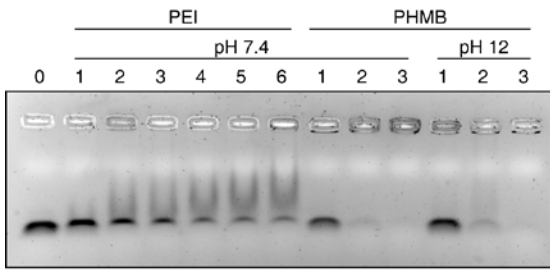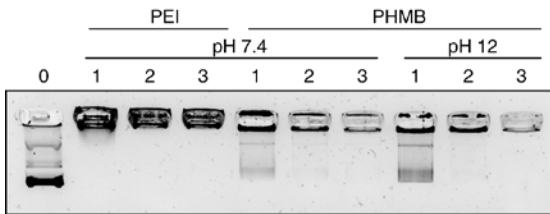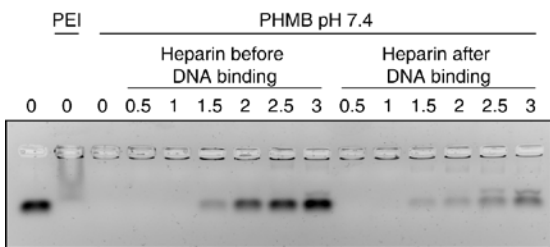
Figure 1. The chemical structure of the free-base form of the biocide poly(hexamethylene biguanide) (PHMB) [1-column]
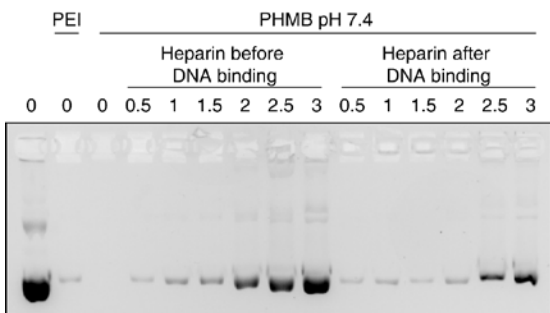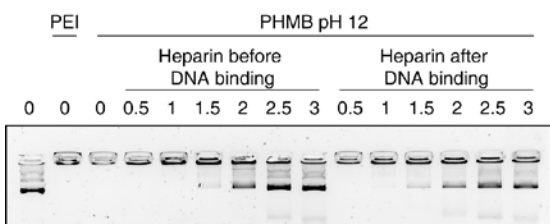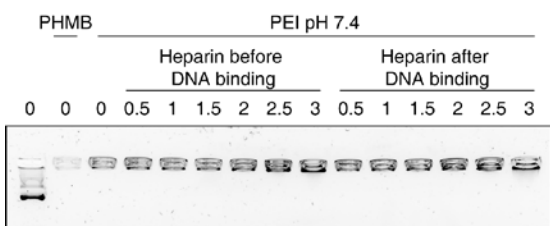
A ODNs

B pDNA

C ODNs

D pDNA

E pDNA

F pDNA

Figure 2. Gel retardation assay for DNA polyplexes of PEI or PHMB at pH 7.4 or pH 12 **(A)** oligodeoxynucleotides **(B)** pEGFP-N1 plasmid DNA **(C)** heparin displacement assay for ODNs at pH 7.4 **(D)** heparin displacement assay for pEGFP-N1 plasmid DNA at pH 7.4 **(E)** heparin displacement assay for pEGFP-N1 plasmid DNA at pH 12 **(F)** heparin displacement assay for pEGFP-N1 plasmid DNA at pH 7.4; (**A-B:** numbers represent polymer/DNA weight ratios, **C-F:** numbers represent heparin/DNA weight ratios, polycation to DNA weight ratio is maintained constant (3:1) except for the first well where no polycation was added) [1-column]
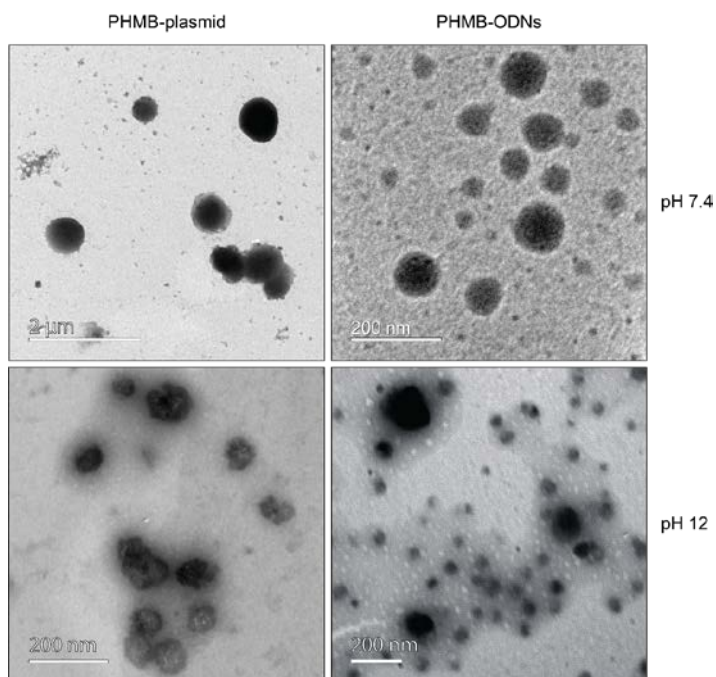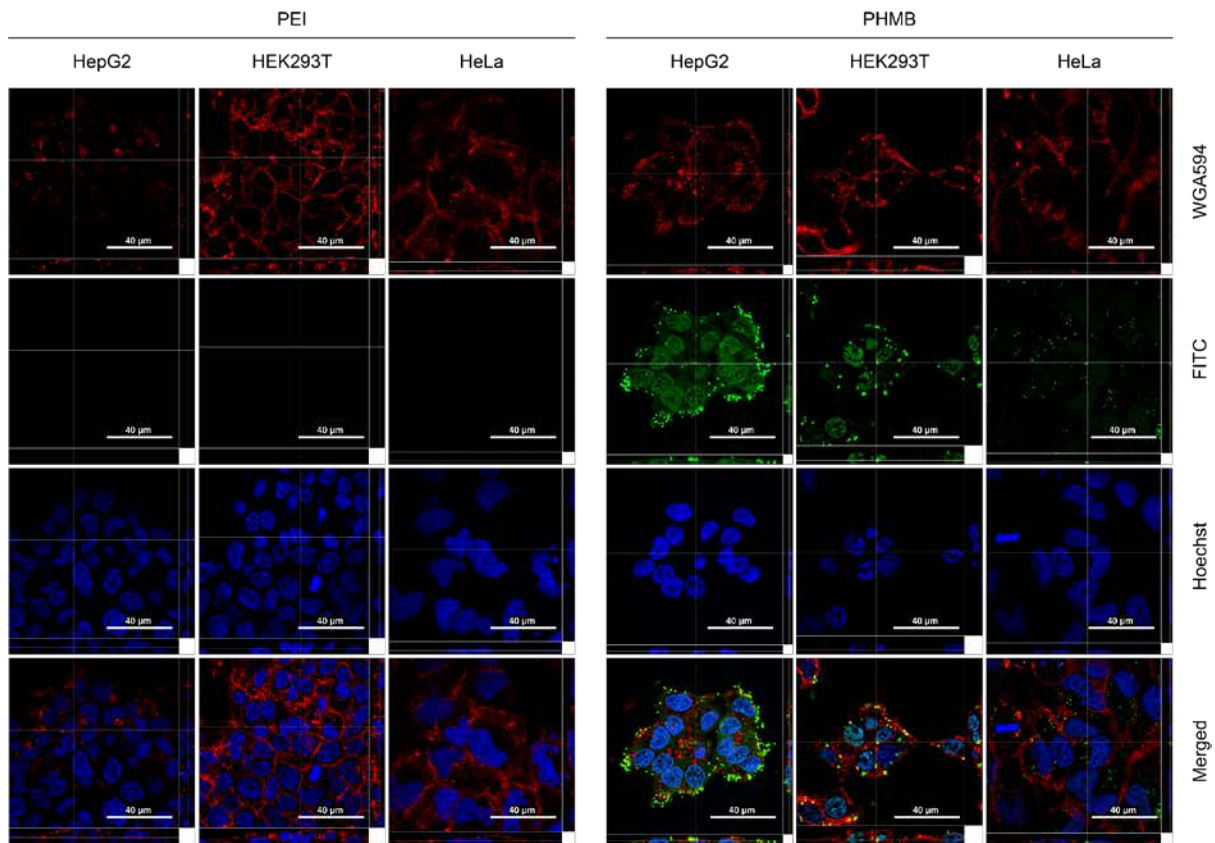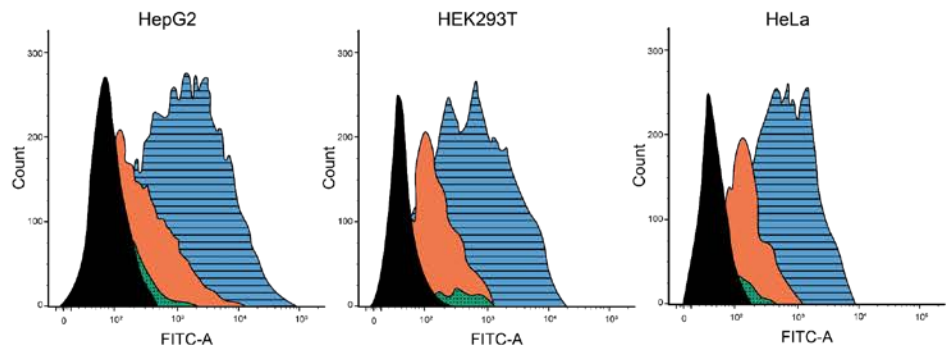

Figure 3. TEM images showing the general microstructure of the polyplexes of PHMB with plasmid DNA or oligodeoxynucleotides (ODNs) at two different pH values (7.4 and 12) [1-column]
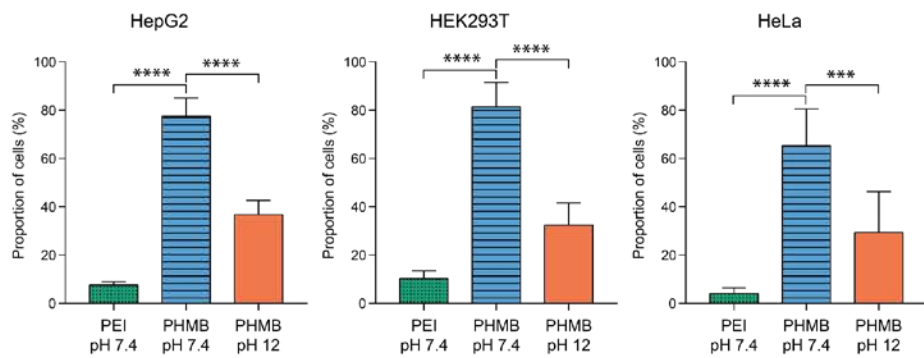
A

B

Control   PEI pH 7.4   PHMB pH 7.4   PHMB pH 12

C

*** p<0.001, **** p<0.0001

Figure 4. (A) Confocal microscopy images showing the difference in cellular uptake of f-ODNs (green, FITC-ODNs) by HepG2, HEK293T, and HeLa. The FITC-ODNs interacted with either PHMB or PEI at pH 7.4 in a weight ratio of 3:1 (polymer:DNA) prior to 24 hours incubation; colours: nuclei – blue (Hoechst 33258), membranes – red (WGA – AlexaFluor™ 594 conjugate) **(B)** Flow cytometry analysis showing difference in cellular uptake of FITC-ODNs by HepG2, HEK293T, and HeLa. The FITC-ODNs were bound to either PHMB or PEI in a 3:1 weight ratio **(C)** Proportion of fluorescent cells measured via flow cytometry following uptake of complexes of PHMB or PEI with FITC-ODNs prepared at different pH values [2-columns]
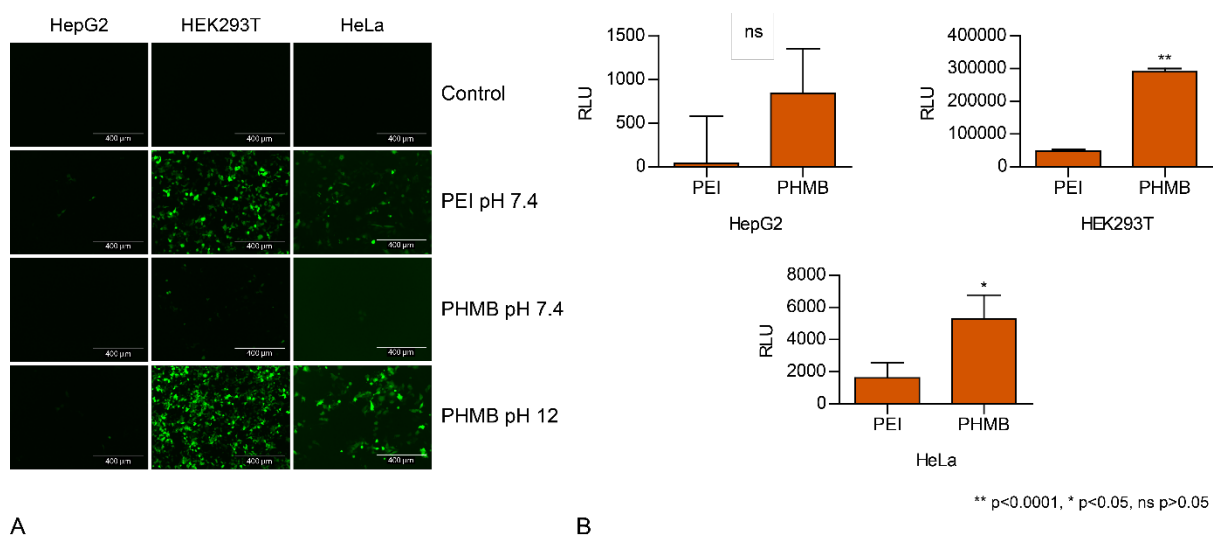

Figure 5. (A) Fluorescence microscopy showing cellular expression of GFP following a three-day exposure of HepG2, HEK293T, and HeLa to polyplexes of pEGFP-N1 plasmid with PEI or PHMB; the PHMB polyplexes self-assembled at two different initial pH conditions (7.4 and 12); bar size – 400 µm **(B)** Relative luminescence measurement of luciferase expression by HepG2, HEK293T, and HeLa following a three-day incubation with polyplexes of pCMV-Luciferase plasmid with either PEI or PHMB; PEI polyplexes self-assembled at pH 7.4, whereas the PHMB polyplexes self-assembled at pH 12 [2-columns]
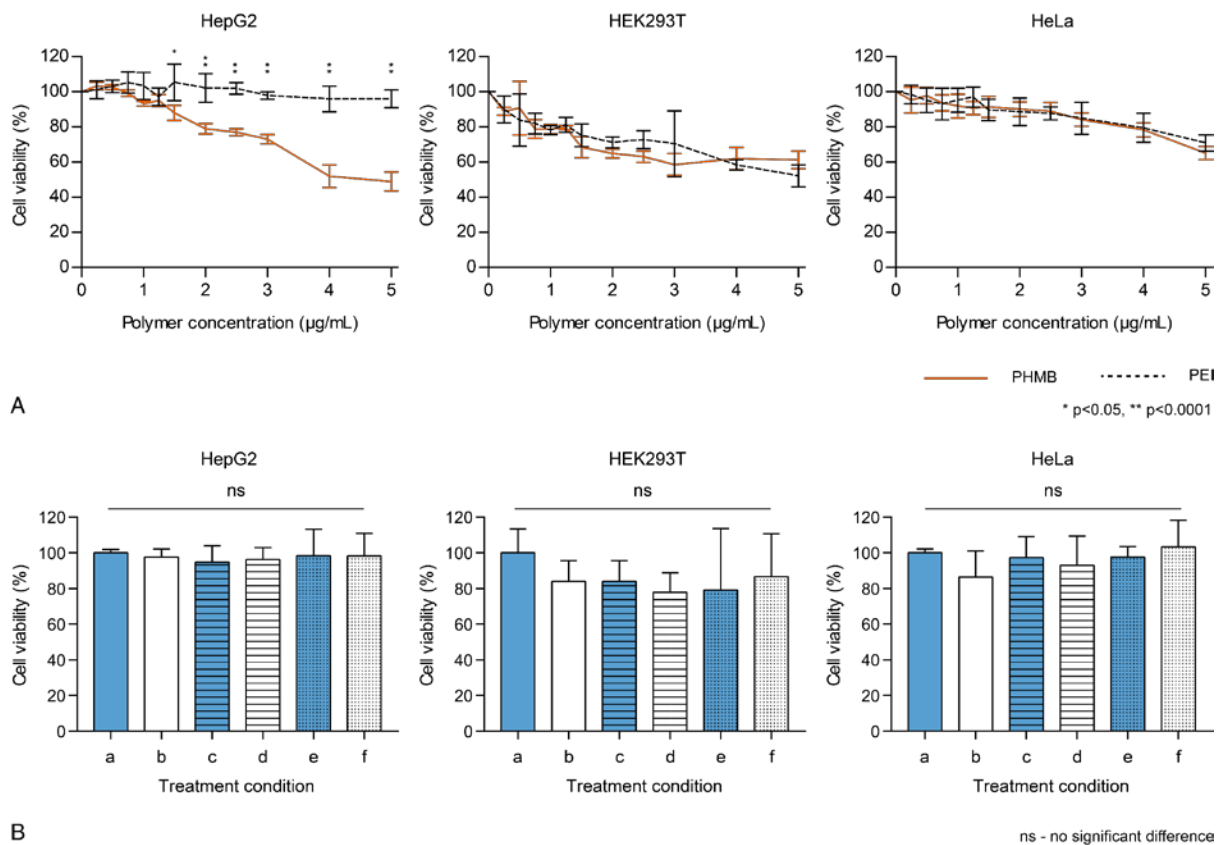
Figure 6. (A) Concentration-dependent decrease in cellular viability after a three-day exposure of HepG2, HEK293T, and HeLa to increasing concentrations of PEI and PHMB (PrestoBlue™ assay) **(B)** Cellular viability of HepG2, HEK293T, and HeLa after a three-day exposure to transfection levels of **a** – PBS pH 7.4, **b** – pH 12 buffer, **c** – 1 µg/mL PHMB in pH 7.4 buffer, **d** – 1 µg/mL PHMB in pH 12 buffer, **e** – 1 µg/mL PHMB complexed in a 3:1 weight ratio with ODNs in pH 7.4 buffer, **f** – 1 µg/mL PHMB complexed in a 3:1 weight ratio to pDNA in pH 12 buffer [2-columns]
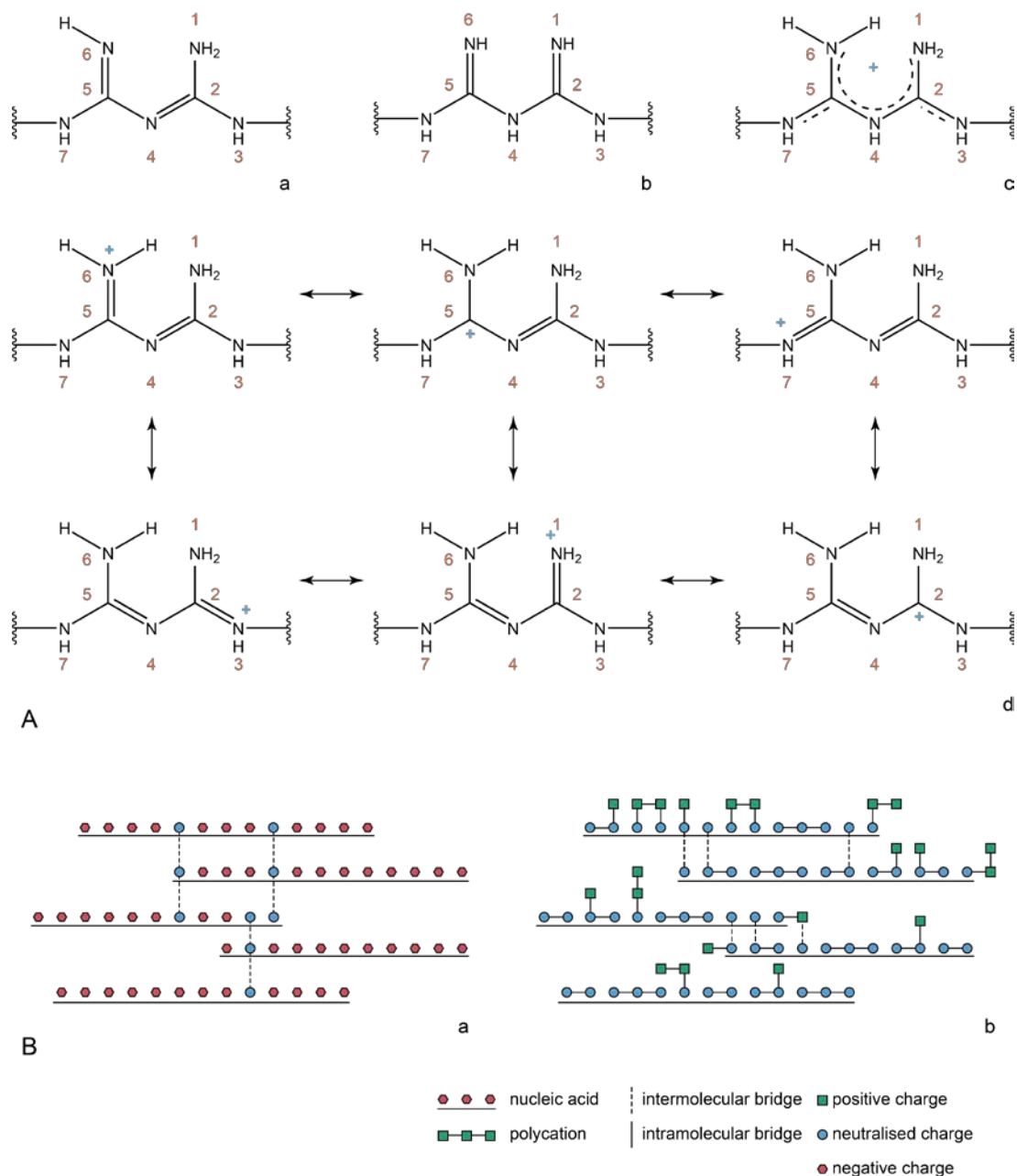
Figure 7. Schematics of **(A)** Resonance structures of the biguanide functional group (A-a) correct iminic representation (A-b) erroneous aminic representation (A-c) mesomeric monoprotonated state (A-d) resonance contributors (reproduced from Maksić & Kovačević [33]) **(B)** The proposed interaction of two polyelectrolytes (polycation and DNA) and formation of inter- and intramolecular bridges at (B-a) low (B-b) high polycation to DNA ratios [2-columns]

Table 1. ζ potential values for polyplexes of PHMB and PEI with plasmid DNA or oligodeoxynucleotides at pH 7.4 or pH 12 (polymer:DNA w/w 3, n=3 replicates)

	Plasmid DNA		ODNs	
	pH 7.4	pH 12	pH 7.4	pH 12
PHMB	34.1 ±3.1 mV	12.3 ±1.8 mV	29.7 ±0.5 mV	9.7 ±0.5 mV
PEI	38.4 ±1.3 mV		35.1 ±1.8 mV	

Table 2. Particle size and PDI values associated with the DLS measurements of particle hydrodynamic diameters for complexes of PHMB and PEI with various concentrations of plasmid DNA or oligodeoxynucleotides at pH 7.4 or pH 12 (polymer:DNA w/w 3, n=3 replicates)

		Plasmid DNA						ODNs			
		pH 7.4			pH 12			pH 7.4		pH 12	
		16 µg/mL	8 µg/mL	4 µg/mL	16 µg/mL	8 µg/mL	4 µg/mL	3 µg/mL	1.5 µg/mL	3 µg/mL	1.5 µg/mL
PHMB	Diameter (nm)	1040 ±35	587 ±79	568 ±46	505 ±26	530 ±6	406 ±14	561 ±28	254 ±10	184 ±5	170 ±8
	PDI	0.22 ±0.05	0.15 ±0.08	0.21 ±0.04	0.19 ±0.02	0.18 ±0.04	0.09 ±0.06	0.09 ±0.03	0.08 ±0.04	0.07 ±0.01	0.08 ±0.05
PEI	Diameter (nm)	590 ±47	349 ±27	352 ±20				653 ±46	280 ±6		
	PDI	0.17 ±0.02	0.07 ±0.04	0.16 ±0.06				0.07 ±0.01	0.08 ±0.01		